Enhanced nuclear level decay in hot dense plasmas

G. Gosselin and P. Morel
Département de Physique Théorique et appliquée, Service de Physique Nucléaire, Commissariat à l'énergie atomique, Boite Postale 12, 91680 Bruyères-le-Châtel, France
(Received 15 April 2004; published 10 December 2004)

A model of nuclear level decay in a plasma environment is described. Nuclear excitation and decay by photon processes, nuclear excitation by electron capture, and decay by internal conversion are taken into account. The electrons in the plasma are described by a relativistic average atom model for the bound electrons and by a relativistic Thomas-Fermi-Dirac model for the free electrons. Nuclear decay of isomeric level may be enhanced through an intermediate level lying above the isomer. An enhanced nuclear decay rate may occur for temperatures far below the excitation energy of the transition to the intermediate level. In most cases, the enhancement factor may reach several decades.

DOI: 10.1103/PhysRevC.70.064603 PACS number(s): 23.20.Nx

In a hot dense plasma, either laser heated or of astrophysical interest [1–3], nuclei in an isomeric state may have a decay rate different from the laboratory value. The large number of photons and free electrons modifies the environment in which the nucleus naturally decays under laboratory conditions through spontaneous emission and internal conversion (IC). In the plasma, the IC decay rate can be modified by the lower number of available electrons in the partially ionized atom. Moreover, new decay modes also appear such as induced photon emission, free electron scattering, or bound internal conversion.

Furthermore, indirect decay channels may be opened, if there exists a nuclear level lying above the isomeric level that may be excited from the isomeric state, and then decay down to the ground state. At first glance, one may expect that this indirect decay mode may become significant when the temperature is around the energy difference between the isomeric level and the upper level. However, if the multipolarities of the excitation transition of the intermediate level and of its decay are more favorable than that of the isomeric transition, one may expect that the indirect decay mode becomes predominant at a lower temperature.

This indirect process would be a valuable tool for investigating nuclear excitation in plasmas. In a laser heated plasma, it could provide experimental conditions allowing tests of the nuclear transition rate model as well as the ability to reach significantly populated higher energy nuclear levels. These studies are critical for nuclear energy storage on an isomeric level and its release mechanism.

If these hot plasmas are maintained for a long enough duration at the thermodynamic equilibrium at a temperature T, the different nuclear level populations reach an equilibrium given by the Boltzmann law where the ratio between any two populations N_i and N_f is easily calculated:

$$\frac{N_f}{N_i} = \frac{2J_f + 1}{2J_i + 1} e^{-(E_f - E_i)/k_B T} \tag{1}$$

where k_B is the Boltzmann constant, E_i and E_f the excitation energies, and J_i and J_f the spins of lower initial state i and the upper final state f.

One remarkable feature of the thermodynamic equilibrium is that the populations can be calculated without any explicit knowledge of the detailed excitation and decay processes. However, in the case of plasmas where only the nuclear populations are not at equilibrium, it gives a strong incentive to simultaneously evaluate each excitation process with its associated decay process. According to the principle of detailed balance, the excitation rate λ_e from state i to state f and the reciprocal decay rate λ_d are related by

$$\frac{\lambda_e}{\lambda_d} = \frac{2J_f + 1}{2J_i + 1} e^{-(E_f - E_i)/k_B T}. \tag{2}$$

Contrary to the case of most astrophysical plasmas, a laser heated plasma will not live long enough for the Boltzmann equilibrium to be reached. Evaluating this equilibration time mandates the evaluation of the nuclear transition rate of every significant microscopic process within the timeframe of the plasma involving every nuclear state that might be populated.

Such studies have been undertaken for a long time [4,5] but seem to get a renewed interest with the recent advent of high-intensity laser sources [6–9]. It is now possible to create plasmas with a lifetime as long as a few nanoseconds and temperatures around several keV. If one considers inertial fusion targets, the temperature might be ten times higher. In such conditions, a significant number of isomers may decay through the indirect channel. If the energy of the isomer is released fast enough, it might be used to heat the neighboring plasma and induce a heat wave able to decay more isomers. The model presented in this paper may give us hints to the properties of the isomeric nucleus needed for the controlled release of energy stored on an isomeric level.

Various excitation processes have already been identified [10]. The main couples of excitation and decay electromagnetic processes are photon absorption and photon emission (both spontaneous and induced); nuclear excitation by electron capture (NEEC), where a free electron is captured on an empty state of an atomic shell, and IC; inelastic and superelastic electron scattering; and nuclear excitation by electron transition (NEET) [11] and bound internal conversion (BIC).

NEET is a resonant process where an electron on a loosely bound shell decays down to an inner shell. If the energy difference between the two atomic shells matches that of a nuclear transition, the nucleus may be excited.

With the existing high-intensity lasers, or with the future facilities being built, high-Z plasmas may be created with a temperature ranging between 10 eV and 10 keV. In these plasmas, the temperature rarely exceeds the excitation energy of nuclear levels higher than the first excited one. When the NEET resonant conditions are not fulfilled, the most efficient excitation processes are NEEC and photon absorption. If we content ourselves with the hypothesis that the electrons are at thermodynamic equilibrium within this range of temperature, the population of electrons having a kinetic energy greater than the nuclear energy transition is usually rather small. Therefore, the inelastic electron scattering excitation rate will not significantly contribute to the total excitation rate because of this threshold energy.

Under those thermodynamic conditions as quoted above, many electrons are free, but there still exist some bound electrons on the inner shells. For strongly converted nuclear transitions, this means that IC remains an important decay process and that excitation occurs through NEEC, as the electronic shells are able to capture a free electron. In those temperature regions, the physical features of the electronic shells vary greatly with the thermodynamic conditions, as the screening effects highly depend on the number of bound electrons. Hence, a correct evaluation of the nuclear transition rate by NEEC and IC must take into account a detailed description of the atom.

In this work, a model coupling both the calculation of the NEEC process and a description of the atom dependence on the thermodynamic conditions of the plasma is presented. Results about several nuclei will show the NEEC dependence on the population of the orbital where the free electron is captured. This model will be used to deal with isomer decay in the plasma. We will then focus on the isomer indirect decay process which involves both an excitation and a decay process.

I. NUCLEAR EXCITATION BY ELECTRON CAPTURE AND INTERNAL CONVERSION IN A PLASMA

NEEC is a resonant process in which a free electron is captured into a bound atomic state and gives a part of its energy to excite a nuclear state. It is the inverse process of the well-known internal conversion. This process was first quoted by Goldanskii and Namiot [12] in 1976, who estimated a very simplistic probability of NEEC in a plasma. Doolen [4,5] then proposed a more sophisticated approach by coupling an internal conversion model with an average atom model. A study of the NEEC process in solid matter has been proposed in the frame of channeling experiments [13–15]. In those experiments, a fully stripped ion beam is channeled within a plane of a crystal to avoid nuclear interactions. It may then capture electrons from the crystal. Some of those captures lead to excitation via a NEEC process. Simplified theoretical models [13–15] have been developed around those experiments, but they may not be extrapolated to plasmas. A more sophisticated theoretical model [16], while it may more easily be extrapolated to plasmas, shows several orders of magnitude discrepancies with the other models. In any case, definitive experimental evidence of NEEC existence remains to be observed.

In the model presented in this paper, we will always assume that the local thermodynamic equilibrium (LTE) is achieved for the electron and photon populations, but not for the nuclear levels populations. This will allow us to derive the expressions for the nuclear transition rates that satisfy the principle of detailed balance seen above in Eq. (2).

The model developed in this work focuses on deriving simultaneously the nuclear excitation and decay rates taking into account the atomic wave functions evaluated by an average atom model at a given temperature and density. It includes a detailed treatment of the electronic transition, which becomes necessary when the free electron kinetic energy is close to the nuclear transition energy.

A. NEEC rate

To excite a nuclear transition of energy ΔE, the free electron, which is captured into an atomic state of binding energy E_b must have a kinetic energy E_r given by

$$E_r \approx \Delta E - |E_b|. \tag{3}$$

This matching condition needs only to be met within an energy interval given by the width of the final state. According to the Fermi golden rule [17], the NEEC cross section for a free electron of kinetic energy E may be written

$$\sigma_{\mathrm{NEEC}}(E) = \frac{2\pi}{\hbar v}|\langle \psi_f \varphi_b | H | \psi_i \varphi_r \rangle|^2 \rho_b(E), \tag{4}$$

where v is the free electron velocity, ψ_i and ψ_f the nuclear wave functions of the initial and final states, φ_r the free electron wave function, and φ_b the bound atomic state wave function. H is the interaction Hamiltonian operator used in the internal conversion theory [18], which contains a Coulomb term and a virtual photon exchange term. This matrix element is the product of a nuclear matrix element in which the radial term contains an integration over r^L (where L is the multipolarity of the nuclear transition) and an atomic matrix element in which the radial term contains an integration over r^{-L-1}. It contains a summation over every atomic state in the atomic shell. Therefore, the final state density $\rho_b(E)$ may be written

$$\rho_b(E) = (2J_f + 1) g(E - E_r), \tag{5}$$

where g is the line shape of the transition. It is centered around the resonance energy E_r.

To obtain a NEEC excitation rate in the plasma, we need the free electron distribution function:

$$f(E) = n(E) f_{\mathrm{FD}}(E), \tag{6}$$

where $n(E)$ is the electronic state density and $f_{\mathrm{FD}}(E)$ the Fermi-Dirac statistics function. The NEEC rate is then obtained by summing over all free electron energies that allow the capture:

$$\lambda_e^{\mathrm{NEEC}} = \int_0^{\Delta E} \sigma_{\mathrm{NEEC}}(E) v(E) f(E) P_b(E) dE, \tag{7}$$

where $P_b(E)$ is the proportion of empty sites in the bound state:

$$P_b(E) = 1 - f_{\mathrm{FD}}(E - \Delta E). \tag{8}$$

The matrix element involved in Eq. (4) must be evaluated by using the electronic wave functions in the thermodynamic conditions of the plasma. The results shown in this work are based on a relativistic average atom model [19,20]. This model solves the Dirac-Fock equation for bound electrons, assuming the atom is in a box with a radius dictated by the plasma density. The electronic populations are treated statistically with a Fermi-Dirac distribution. The relativistic feature is necessary because the atomic properties for heavy ions and the internal conversion coefficients cannot be accurately calculated in a classical model, because they strongly depend on the wave function behavior inside the nucleus.

In this work, a more sophisticated atom model detailing the individual configurations is usually not necessary. With such models, the NEEC and IC transition rates would be summed up over every configuration. However, as every term involved in the transition rates calculations, except the line shape g, varies slowly with the binding energy of the captured electron, it can be safely assumed that these terms can be factorized out of the integral in Eq. (7) and replaced by their value in the average atom model.

The line shape of the electronic transition needs a more detailed treatment, especially when the resonant energy E_r is close to the limits of the integral (7). The huge number of different configurations precludes any exact calculations and so only a statistical approach can be used. This high number of configurations implies closely spaced individual transitions [21] with their own width leading to a strong overlap. So, we will replace the summation over every single transition linewidth by a statistically broadened averaged transition approximated by a Gaussian distribution [22–26]. We naturally assume that it lies between the continuum and the average atom shell where the electron is captured. So we express the line shape g:

$$g(E - E_r) = \frac{1}{\sqrt{2\pi\varepsilon^2}} e^{-(E - E_r)^2/2\varepsilon^2}, \tag{9}$$

where ε is the dispersion of the electronic transition energy of the real configuration around the average atom value [24], issued from the classical theory of fluctuations [27].

No explicit Doppler effect is taken into account. However, in the plasma, the electrons move much faster than the ions. Therefore, for a given ion in the laboratory frame, the free electron distribution function is nearly constant inside the energy interval of width ε around E_r.

The final NEEC rate is expressed as

$$\lambda_e^{\mathrm{NEEC}} = \frac{2\pi}{\hbar} n(E_r) |\langle \psi_f \varphi_b | H | \psi_i \varphi_r \rangle|^2 (2J_f + 1) f_{\mathrm{FD}}(E_r) \times [1 - f_{\mathrm{FD}}(E_b)] \frac{1}{2} \left[\mathrm{erf}\left(\frac{E_r}{\varepsilon\sqrt{2}} \right) - \mathrm{erf}\left(\frac{E_b}{\varepsilon\sqrt{2}} \right) \right], \tag{10}$$

where erf is the usual notation for the error function, defined by

$$\mathrm{erf}(x) = \int_0^x e^{-t^2} dt. \tag{11}$$

The hypothesis on the line shape is only necessary when the average atom binding energy is close to the nuclear transition energy. In that case, some of the individual transitions may not occur as they may have an energy larger than the nuclear transition energy, and thus, according to Eq. (3), are prohibited from NEEC interaction. When not in that situation, the expression (10) reduces to

$$\lambda_e^{\mathrm{NEEC}} = \frac{2\pi}{\hbar} n(E_r) |\langle \psi_f \varphi_b | H | \psi_i \varphi_r \rangle|^2 (2J_f + 1) f_{\mathrm{FD}}(E_r) \times [1 - f_{\mathrm{FD}}(E_r - \Delta E)]. \tag{12}$$

This expression can also be directly derived from Eq. (7) if the line shape g is taken to be a Dirac distribution. This is equivalent to considering that the average atom model fully applies, and that the electronic transition occurs between a free state and a fixed energy bound state.

B. Internal conversion rate

For an isolated neutral atom with a fully occupied atomic shell, the internal conversion rate λ_{IC} can be written with the Fermi golden rule [17]:

$$\lambda_{\mathrm{IC}} = \frac{2\pi}{\hbar} |\langle \psi_i \varphi_r | H | \psi_f \varphi_b \rangle|^2 \rho_r(E_r), \tag{13}$$

where $\rho_r(E_r)$ is the final state density:

$$\rho_r(E_r) = (2J_i + 1) n(E_r). \tag{14}$$

The matrix element in Eq. (13) is the conjugate of the matrix element in Eq. (4).

In a plasma, the internal conversion rate λ_d^{IC} must take into account the probability of presence of the electron on the converted atomic shell as well as the probability of finding an empty site in the continuum. It then can be expressed as

$$\lambda_d^{\mathrm{IC}} = \frac{2\pi}{\hbar} |\langle \psi_i \varphi_r | \mathrm{H} | \psi_f \varphi_b \rangle|^2 \rho_r(E_r) \frac{f(E_b)}{2J_b + 1} [1 - f_{\mathrm{FD}}(E + \Delta E)], \tag{15}$$

where $f(E_b)$ is the distribution function of the bound electron. It has been divided by $2J_b+1$ to get the proportion of present electrons on the shell. It contains the same lineshape as expressed in Eq. (9). The IC plasma rate is then obtained by integrating over the energy of the electronic bound state. The final nuclear decay rate becomes

$$\lambda_d^{\mathrm{IC}} = \frac{2\pi}{\hbar} n(E_r) |\langle \psi_i \varphi_r | H | \psi_f \varphi_b \rangle|^2 (2J_i + 1) f_{\mathrm{FD}}(E_b) \times [1 - f_{\mathrm{FD}}(E_r)] \frac{1}{2} \left[\mathrm{erf}\left(\frac{E_r}{\varepsilon\sqrt{2}} \right) - \mathrm{erf}\left(\frac{E_b}{\varepsilon\sqrt{2}} \right) \right]. \quad (16)$$

C. Internal conversion coefficient evaluation

The neutral atom internal conversion rate is closely related to the internal conversion coefficient:

$$\lambda_{\mathrm{IC}} = \frac{\alpha \ln 2}{T^{\gamma}_{J_f \to J_i}}, \quad (17)$$

where $T^{\gamma}_{J_f \to J_i}$ is the radiative lifetime of the transition. The nuclear decay rate may then be expressed with the internal conversion coefficient as a function of the thermodynamic conditions in the plasma:

$$\lambda_d^{\mathrm{IC}} = \frac{\alpha(T_e) \ln 2}{T^{\gamma}_{J_f \to J_i}} f_{\mathrm{FD}}(E_b) [1 - f_{\mathrm{FD}}(E_r)] \frac{1}{2} \left[\mathrm{erf}\left(\frac{E_r}{\varepsilon\sqrt{2}} \right) - \mathrm{erf}\left(\frac{E_b}{\varepsilon\sqrt{2}} \right) \right], \quad (18)$$

where T_e is the electronic temperature of the plasma. The nuclear excitation rate is

$$\lambda_{\mathrm{e}}^{\mathrm{NEEC}} = \frac{2J_f + 1}{2J_i + 1} \frac{\alpha(T_e) \ln 2}{T^{\gamma}_{J_f \to J_i}} f_{\mathrm{FD}}(E_r) [1 - f_{\mathrm{FD}}(E_b)] \frac{1}{2} \left[\mathrm{erf}\left(\frac{E_r}{\varepsilon\sqrt{2}} \right) - \mathrm{erf}\left(\frac{E_b}{\varepsilon\sqrt{2}} \right) \right]. \quad (19)$$

The ratio of the NEEC excitation rate to the internal conversion decay rate is in accordance with the principle of detailed balance as expressed in Eq. (2):

$$\frac{\lambda_e^{\mathrm{NEEC}}}{\lambda_d^{\mathrm{IC}}} = \frac{2J_f + 1}{2J_i + 1} e^{-\Delta E / k_B T}. \quad (20)$$

The internal conversion coefficient calculations have been carried out with a model taking into account the finite nuclear size, the electronic screening effects, and the dynamic effects of the interaction between the electron shells and the nuclear charge. They are based upon the model exposed by Pauli [18,28,29] and use a purposely modified version of the CATAR code [30], which uses external wave functions extracted from the average atom model, as described above.

D. Photon excitation and decay process

Another important nuclear excitation process is through the absorption of photons. The corresponding decay processes are spontaneous and induced emission. This last process becomes predominant when the photon temperature becomes higher than the nuclear energy transition. These radiative transition rates are calculated with a photon population at the thermodynamic equilibrium, that is, a blackbody population. Therefore, they only depend on the temperature, not the density.

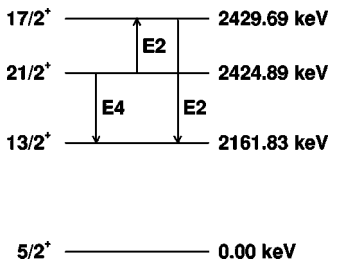

FIG. 1. Simplified level scheme of molybdenum-93.

For a nuclear transition of energy ΔE between a lower nuclear state i and a higher nuclear state f, the excitation rate is given by

$$\lambda_{\mathrm{e}}^{\gamma} = \frac{2J_f + 1}{2J_i + 1} \frac{\ln 2}{T^{\gamma}_{J_f \to J_i}} \frac{1}{e^{\Delta E / k_B T} - 1}, \quad (21)$$

and the total (spontaneous and induced) decay rate is

$$\lambda_{\mathrm{d}}^{\gamma} = \frac{\ln 2}{T^{\gamma}_{J_f \to J_i}} \frac{e^{\Delta E / k_B T}}{e^{\Delta E / k_B T} - 1}. \quad (22)$$

These photon excitation and decay rates follow the principle of detailed balance.

II. Results

A. Transition rates

The model exposed in Sec. I may be used to evaluate the transition rates in a plasma for any nuclear transition whose lifetime is known. As a first case, we will consider the excitation of the first excited level in molybdenum-93 built on the isomeric level. It lies at 4.8 keV above the isomeric level, which itself lies 2424.89 keV above the ground level (a simplified level scheme is shown below on Fig. 1). It can be excited via an $E2$ transition. Under laboratory conditions, it mainly decays through IC on the L and M atomic shells.

Figure 2 shows the internal conversion coefficient of this transition as a function of temperature at several densities for the $E2$ transition built on the isomeric level. The IC coeffi-

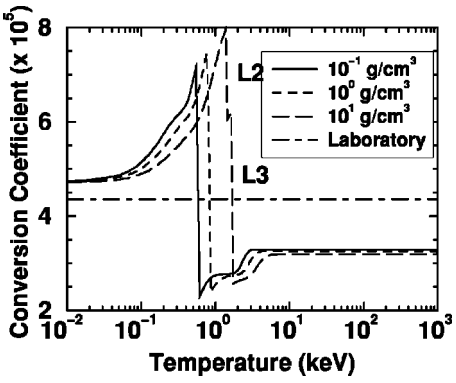

FIG. 2. Internal conversion coefficient for the 4.8 keV $E2$ transition in molybdenum-93.

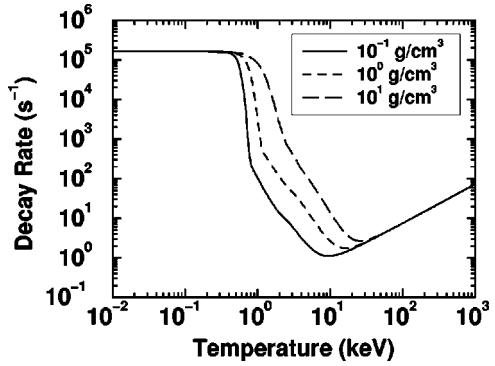

FIG. 3. Nuclear decay rate by internal conversion and by photon emission for the 4.8 keV $E2$ transition in molybdenum-93.

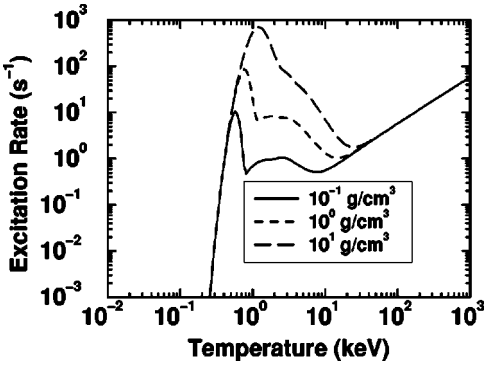

FIG. 4. Nuclear excitation rate by NEEC and photon absorption for the 4.8 keV $E2$ transition in molybdenum-93.

cient calculations under laboratory conditions have been performed with the built-in potential provided with the CATAR code [30]. At low temperature, the IC coefficient is constant and close to its laboratory value evaluated at 4.36×10^5. The slight difference comes from the different models of potential adopted under laboratory conditions and in the plasma at a temperature where the average atom model is not a perfect description.

When temperature increases, the atom is progressively ionized, and the remaining bound electrons are less screened from the nucleus Coulombian potential. The atomic shells are more tightly bound and the overlap between the atomic wave function and the nuclear wave function is stronger, resulting in an IC coefficient increase. Some abrupt drops occur when the binding energy of an atomic shell increases above the nuclear transition energy, thus prohibiting the internal conversion. In molybdenum-93, the atomic shells $L1$, $L2$, and $L3$ follow this behavior at temperatures ranging between 0.7 keV and 1.7 keV.

When density increases, the volume available for the free electrons between the atoms decreases. So the ionization of the atom becomes more difficult as temperature increases. Thus, the decrease of the screening effects and the increase of the binding energy occur at higher temperatures and so do the abrupt drops of the IC coefficient.

The nuclear decay rate for the $E2$ transition above the isomeric level of molybdenum-93 is shown in Fig. 3. The decay rates feature the sum of the IC decay rate and the photon spontaneous and induced emissions. For every density, the decay rate is constant at low temperatures at approximately the laboratory value, and then decreases when the atom is progressively ionized. At higher temperatures, the photon-induced emission becomes the major process, as internal conversion is impeded by the lack of bound electrons, and the transition rate begins to increase.

Between 1 and 10 keV, the L atomic shells ionization occurs and strongly varies with density, as a denser plasma requires a higher temperature for the same ionization fraction. Therefore, at a given temperature, the IC decay rate increases with density. If the IC coefficient was small in front of 1, this effect would be negligible.

The nuclear excitation rate for this transition is shown in Fig. 4. The excitation rates feature the sum of the NEEC excitation rate and photon absorption. The excitation rate is small for low temperatures when the NEEC is inhibited by the fully occupied atomic shells and the low number of free electrons. It increases when the temperature rises up to a maximum after which the kinetic energy of most of the free electrons becomes too high for NEEC. This maximum excitation rate follow the increase of the free electron density.

Thereafter, the only remaining excitation process is photon absorption, which increases with temperature. No sharp drop occurs where the IC coefficient vanishes on some shells. The statistical broadening of the transition lies around 200 eV and so the IC rate smoothly disappears.

The theory developed by Doolen [4,5] is similar in principle to ours. However, it did not include a statistical approach for the atomic transition treatment, relying only on the average atom model. In the case of uranium-237, Fig. 5 shows the excitation rate in both our model and Doolen's and Fig. 6 the decay rate of the same transition. In both figures, the good general agreement between both models is quite obvious, although some of the discrepancies might be attributed to the statistical treatment of the vanishing internal conversion on the M atomic shells.

B. Enhanced nuclear decay of isomers

The next results have all been processed for a generic density of 1 g/cm^3. For each considered transition, the real nuclear matrix element has been used whenever available. In

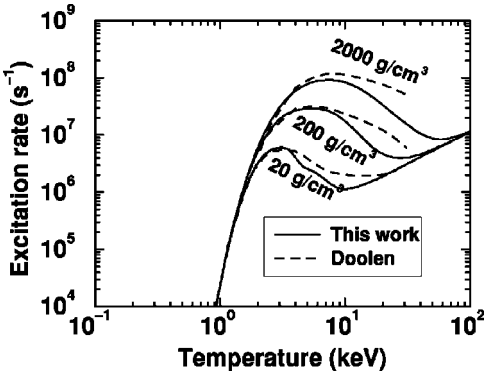

FIG. 5. Nuclear excitation rate by NEEC and photon absorption for the 11.39 keV $M1+E2$ transition of uranium-237.

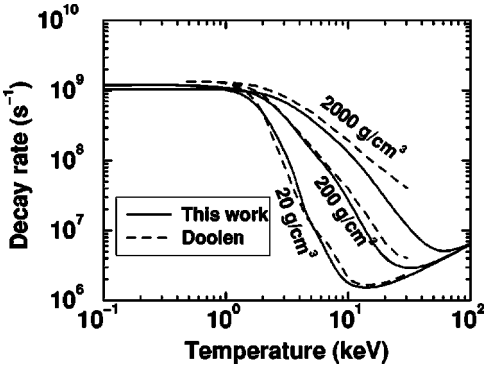

FIG. 6. Nuclear decay rate by internal conversion and photon emission for the 11.39 keV $M1+E2$ transition of uranium-237.

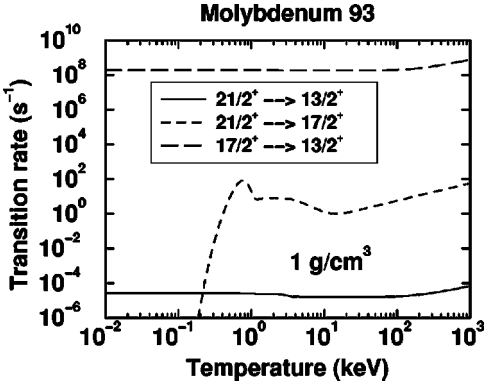

FIG. 7. Natural and indirect transition rates for the $21/2^+$ level in molybdenum-93.

the few cases when it is not, the Weisskopf estimate has been used instead.

Various nuclei possess a nuclear level scheme allowing an isomeric state to decay by an indirect channel. A frequent case occurs when the order of two levels in the same band is reversed. The band built on the ground level $5/2^+$ of molybdenum-93 is one such example whose level scheme was shown above in Fig. 1. The $17/2^+$ and $21/2^+$ levels are inverted, making the $21/2^+$ an isomer with a 6.95 h lifetime.

In a plasma, indirect decay of the isomer may take place through the $17/2^+$ level lying only 4.8 keV above the isomeric level. If the plasma temperature is high enough, this process may be more efficient than the natural decay of the isomer.

Figure 7 shows in solid line the isomer decay rate via the $E4$ transition, in a short dashed line the excitation of the intermediate level and in a long dashed line the decay of the intermediate level. The isomer direct decay rate always lies between 10^{-5} and 10^{-4} s^{-1}, corresponding to a lifetime of a few hours. The excitation rate of the intermediate level is totally negligible at very low temperatures, but rises very quickly and becomes higher than the isomer direct decay rate around 0.2 keV. From now on, the threshold temperature of an isomeric level is defined by the lowest temperature for which the indirect decay rate equals the direct decay rate. It is lower by a factor of around 20 than the transition energy to the intermediate level. At higher temperatures, it maintains itself between 10^5 and 10^7 higher than the isomer decay rate. As the decay of this intermediate level is always higher than 10^8 s^{-1}, the limiting factor for indirect decay is the excitation of the intermediate level from the isomeric level. So the net decay rate of the isomer has been raised by a factor of 10^5 to 10^7.

The threshold temperature lies in a region where the main atomic shells contributing to IC and NEEC are still fully populated. Therefore, the transition rates are nearly independent on the plasma density, and so is the threshold temperature. The transition energy is usually about one decade higher (as Table I below will show). If the threshold energy lies in a region where the atomic shells begin to be ionized, it could depend on the plasma density. However, the transition would then lie in a region where IC is forbidden because the nuclear transition energy is greater than the binding energy of even the most tightly bound atomic shell. Then, the transition rates only feature the photon transition rate which is independent on the density. Therefore, in most cases, the threshold temperature does not depend on density.

Another example of enhanced nuclear decay is technetium-96. The isomer level is a 4^+ lying 34.28 keV above a 7^+ ground level to which it decays via a $M3$ transi-

TABLE I. Isomer indirect decay.

						Transitions		
Nucleus	E_m (keV)	$T_{1/2}$	T_s (keV)	ΔE (keV)	$\Delta E/T_s$	$m\rightarrow g$	$m\rightarrow e$	$e\rightarrow g$
^{44}Sc	270.95	58.61 h	3.45	78.9	22.9	$E4$	$E2$	$E2$
^{45}Ti	36.74	3.0 μs	0.70	3.0	4.3	$E2$	$M1+E2$	$M1+E2$
^{52}Mn	377.749	21.1 min	11.29	353.9	31.3	$E4$	$E2$	$E2$
^{93}Mo	2424.89	6.85 h	0.22	4.8	21.8	$E4$	$E2$	$E2$
^{96}Tc	34.28	51.5 min	0.38	11.1	29.2	$M3$	$M1$	$E2$
			0.78	14.9	19.1		$E2$	$M1$
^{99}Tc	142.6833	6.01 h	1.68	38.4	22.8	$E3,M4$	$M2$	$M1+E2$
^{202}Pb	2169.84	3.53 h	1.55	38.6	24.9	$E4,E5$	$E2$	$E2$
^{204}Pb	2185.79	67.2 min	3.67	78.5	21.4	$E5$	$E2$	$E3$
^{242}Am	48.60	141 y	0.65	4.1	6.3	$E4$	$E2$	$E2$

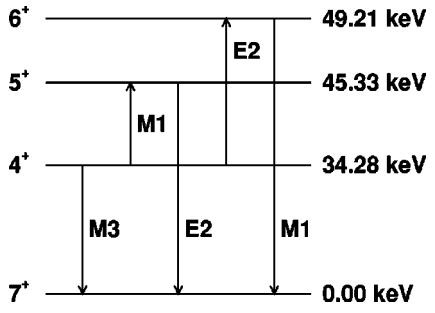

FIG. 8. Low levels of technetium-96.

tion in 51 min. Indirect decay is possible via two different intermediate levels, 5^+ and 6^+, as shown in Fig. 8.

Figure 9 shows the indirect decay via the 5^+ level and Fig. 10 via the 6^+ level. For the 6^+ case, the general behavior is the same as for molybdenum-93. The threshold temperature is once again around 20 times lower than the excitation energy of the intermediate level. At higher temperatures, the indirect decay rate reaches nearly 10^9 times the direct decay rate of the isomer.

The indirect decay via the 5^+ level is a little bit different. The threshold temperature is around 30 times lower than the intermediate level excitation energy. Above a temperature of 2 keV, the decay rate of the intermediate level becomes lower than the excitation rate to this level, and thus limits to an already respectable 10^9 the decay rate enhancement. However, this transition rate configuration allows populating the intermediate level at a faster rate than its decay rate. Therefore, it may be possible to realize a temporary population inversion between the ground level and the intermediate level.

The indirect nuclear level decay effect is present on many isomeric states as shown in Table I. In this table, T_s is the threshold temperature above which indirect decay to the ground level g is faster than natural decay, and ΔE is the nuclear transition energy between the intermediate level denoted e and the isomeric level m.

We can define a decay enhancement factor as the ratio between the indirect and the direct decay rate of the isomeric level. The indirect decay rate is the lower between the excitation rate of the intermediate level and the decay rate of this

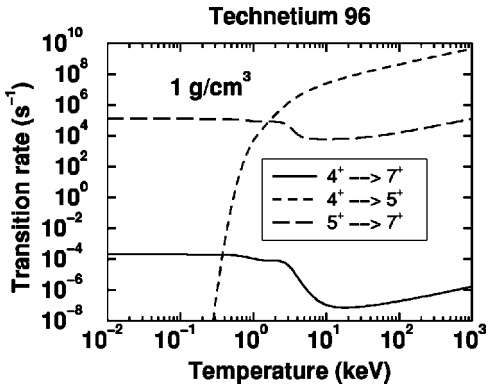

FIG. 9. Indirect decay of the 4^+ level in technetium-96 via the 5^+ level.

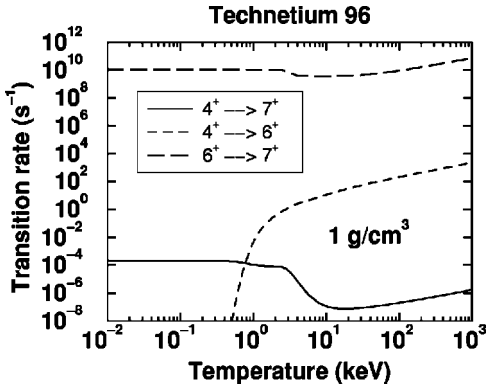

FIG. 10. Indirect decay of the 4^+ level in technetium-96 via the 6^+ level.

intermediate level to the ground state. However, for every case in Table I except for ^{96}Tc via the 5^+ intermediate level, the excitation rate to the intermediate level is the significant rate.

The decay enhancement factors are shown on Figs. 11 and 12 and as a function of temperature for several nuclei. For every nucleus, it increases up to an asymptotic maximum. Before the asymptotic value, in most of the cases, the increase is monotonic, but some nuclei show a structure due to the vanishing of IC on some shells at high temperature. In any case, the asymptotic value is reached at a temperature high enough for NEEC and IC to become negligible in front of the photon transition processes. The decay enhancement factor is then directly correlated to the ratio of the nuclear matrix element of the direct and the indirect transition.

Figure 13 shows the asymptotic enhancement factor as a function of the ratio between the intermediate level excitation energy and the threshold temperature. Only two of the evaluated nuclei have a low ratio. For americium-242, the transition to the intermediate level involves a change in the quantum number K, which greatly hampers the excitation. For titanium-45, the natural decay transition is hardly more difficult than the indirect decay one. That also explains a low asymptotic enhancement factor. Every other nucleus has a transition energy to threshold temperature ratio around 20 or higher. For these nuclei, there is a wide variety of asymptotic enhancement factors related to each individual nuclear property of the nuclear transitions. These can get as high as 10^{13}

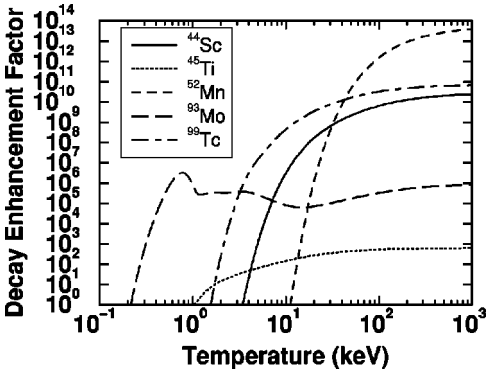

FIG. 11. Decay enhancement factor.

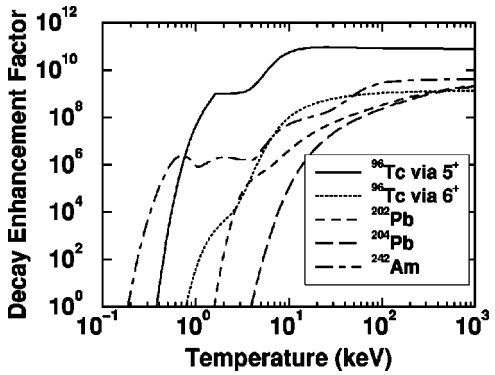

FIG. 12. Decay enhancement factor.

and are never lower than 10^6. The indirect nuclear decay of an isomeric level can be very efficient.

This paper is an application of the ideas of Olariu [31–33] in a context where it had not been considered previously: a hot plasma where the excitation is ruled by thermal free electrons and LTE atomic levels. The indirect isomer decay process in the plasma is identical in its principle to the two-step γ-ray transition from isomeric states described by Olariu, where the indirect decay is induced by an intense photon flux at the appropriate energy. The isomer levels for which this photon induced decay is the most efficient correspond to the plasma cases where the transition energy to threshold temperature ratio and asymptotic enhancement factor are the highest. This result is easily explained by considering that the Planckian photon population in the plasma plays the same role as the incident photon flux.

III. CONCLUSION

In this work, we exposed a model of evaluation of NEEC and IC transition rates in a plasma. It is based on the Fermi golden rule and an atom description by the relativistic average atom model. This model is in a good agreement with the model proposed by Doolen [4,5]. A new detailed description of the electronic transition has been introduced with transition widths issued from a statistical broadening of a single transition equivalent to the numerous individual transitions.

This last feature is the main improvement over the model developed by Doolen [4,5]. It becomes needed whenever the binding energy of the atomic levels onto which the electrons are captured is close to the nuclear excitation energy. Even though NEEC is a resonant process, the average atom model provides a correct description of the atomic level properties. A more detailed description of every possible configuration would involve a summation of excitation rate terms with a slightly different free electron population and energy (within the statistical broadening boundaries). Averaging all those terms to the average atom model value is not too stringent an approximation provided that only the proportion of free electrons whose kinetic energy is less than the atomic level binding energy is taken into account.

However, experimental evidence of the microscopic NEEC phenomenon is still to be observed. An experiment [34] has been scheduled on the GANIL facility and is intended to observe for the first time a NEEC process on a fully stripped ion ^{57}Fe. Other experiments in a plasma environment are also being planned but still have not been finalized.

When a nucleus in an isomeric state is placed within a hot plasma, its decay lifetime may be greatly reduced if there exists a nuclear level a little higher than the isomer that can be reached by a favorable transition. This indirect process can be faster by several orders of magnitude for temperatures that may be one decade lower than the excitation energy. This can open a large field of experiments where the excitation of nuclear transitions becomes possible for temperatures much lower than the transition energy.

This study has been conducted from a theoretical point of view. Experimental constraints, such as the admissible lifetime of the isomer, have not been dealt with in this work, and would have to be taken into account for conceiving an experimental setup.

Theoretical work remains to be done, as two other electromagnetic nuclear excitation processes have not been considered. For the higher temperatures, when most of the electrons are free, inelastic electron scattering may become a dominant process. However, most of the threshold temperatures found in this work are not high enough for this excitation process to have a significant influence. A more complex excitation process is NEET, with its corresponding decay process BIC. It may play an important part in indirect decay whenever the energy of the involved transitions approximately matches an atomic transition energy.

The nuclear indirect decay process may be a good tool for investigating nuclear excitation in a plasma as it gives access to higher transition energies than the temperature of the plasma, as well as giving a relatively easy way to measure the excitation rate with the remaining isomer population.

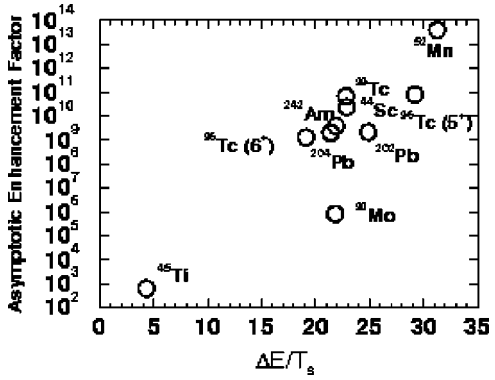

FIG. 13. Asymptotic enhancement factor.

[1] M. Schumann, F. Käppeler, R. Böttger, and H. Schölermann, Phys. Rev. C **58**, 1790 (1998).
[2] R. A. Ward and W. A. Fowler, Astrophys. J. **238**, 266 (1980).
[3] J. J. Carroll, J. A. Anderson, J. W. Glesener, C. D. Eberhard, and C. B. Collins, Astrophys. J. **344**, 454 (1989).
[4] G. D. Doolen, Phys. Rev. C **18**, 2547 (1978).
[5] G. D. Doolen, Phys. Rev. Lett. **40**, 1695 (1978).
[6] A. V. Andreev *et al.*, Zh. Eksp. Teor. Fiz. **118** 1343 (2000) [JETP **91** 1163 (2000)].
[7] A. V. Andreev, A. K. Van'kov, K. Yu. Platonov, Yu. V. Rozdestvenskiĭ, S. P. Chizhov, and V. E. Yashin, Zh. Eksp. Teor. Fiz. **121**, 1004 (2002) [JETP **94**, 862 (2002)].
[8] J. J. Niez, C. R. Phys. **3**, 1255 (2002).
[9] J. J. Niez and P. Averbuch, Phys. Rev. C **67**, 024611 (2003).
[10] M. R. Harston and J. F. Chemin, Phys. Rev. C **59**, 2462 (1999).
[11] P. Morel, V. Méot, G. Gosselin, D. Gogny, and W. Younes, Phys. Rev. A **69**, 063414 (2004).
[12] V. I. Goldanskii and V. A. Namiot, Phys. Lett. **62B**, 393 (1976).
[13] J. C. Kimball, D. Bittel, and N. Cue, Phys. Lett. A **152**, 367 (1991).
[14] N. Cue, Nucl. Instrum. Methods Phys. Res. B **40/41**, 25 (1989).
[15] N. Cue, J. C. Poizat, and J. Remillieux, Europhys. Lett. **8**, 19 (1989).
[16] Zhu-Shu Yuan and J. C. Kimball, Phys. Rev. C **47**, 323 (1993).
[17] A. Messiah, *Quantum Mechanics* (North Holland, Amsterdam, 1961).
[18] W. D. Hamilton, *The Electromagnetic Interaction in Nuclear Spectroscopy* (North Holland, Amsterdam, 1975).
[19] B. F. Rozsnyai, Phys. Rev. A **5**, 1137 (1972).
[20] D. A. Liberman, Phys. Rev. B **20**, 4981 (1979).
[21] H. R. Griem, *Spectral Line Broadening by Plasmas* (Academic Press, New York, 1977).
[22] G. Faussurier, C. Blancard, and A. Decoster, J. Quant. Spectrosc. Radiat. Transf. **58**, 571 (1997).
[23] G. Faussurier, C. Blancard, and A. Decoster, Phys. Rev. E **56**, 3474 (1997).
[24] G. Faussurier, C. Blancard, and A. Decoster, Phys. Rev. E **56**, 3488 (1997).
[25] F. Perrot, Physica A **150**, 357 (1988).
[26] S. J. Rose, J. Phys. B **25**, 1667 (1992).
[27] L. Landau and E. Lifchitz, *Physique Statistique* (Mir, Moscow, 1985).
[28] H. C. Pauli, Helv. Phys. Acta **40**, 713 (1967).
[29] H. C. Pauli, Z. Phys. **202**, 255 (1967).
[30] H. C. Pauli and U. Raff, Comput. Phys. Commun. **9**, 392 (1975).
[31] S. Olariu, A. Olariu, and V. Zoran, Phys. Rev. C **56**, 381 (1997).
[32] S. Olariu and A. Olariu, Phys. Rev. C **58**, 333 (1998).
[33] S. Olariu and A. Olariu, Phys. Rev. C **58**, 2560 (1998).
[34] GANIL proposal, accepted in January 2003.